Title
The pGinger Family of Expression Plasmids

Journal
Microbiology Spectrum, 11(3)

ISSN
2165-0497

Authors
Pearson, Allison N
Thompson, Mitchell G
Kirkpatrick, Liam D
et al.

Publication Date
2023-06-15

DOI
10.1128/spectrum.00373-23

Peer reviewed

AMERICAN SOCIETY FOR MICROBIOLOGY | Microbiology Spectrum

RESOURCE REPORT

The pGinger Family of Expression Plasmids

Allison N. Pearson,[a,b,c] Mitchell G. Thompson,[a,d] Liam D. Kirkpatrick,[a,d] Cindy Ho,[a,b] Khanh M. Vuu,[a,d] Lucas M. Waldburger,[a,b,e] Jay D. Keasling,[a,b,f,g,h] Patrick M. Shih[a,c,d,i]

[a]Joint BioEnergy Institute, Emeryville, California, USA
[b]Biological Systems & Engineering Division, Lawrence Berkeley National Laboratory, Berkeley, California, USA
[c]Department of Plant and Microbial Biology, University of California, Berkeley, California, USA
[d]Environmental Genomics and Systems Biology Division, Lawrence Berkeley National Laboratory, Berkeley, California, USA
[e]Department of Bioengineering, University of California, Berkeley, California, USA
[f]Department of Chemical and Biomolecular Engineering, University of California, Berkeley, California, USA
[g]The Novo Nordisk Foundation Center for Biosustainability, Technical University of Denmark, Kongens Lyngby, Denmark
[h]Center for Synthetic Biochemistry, Institute for Synthetic Biology, Shenzhen Institutes for Advanced Technologies, Shenzhen, China
[i]Innovative Genomics Institute, University of California, Berkeley, California, USA

Allison N. Pearson and Mitchell G. Thompson contributed equally to this article. The order of co-first authors was determined by who has the reddest hair.

ABSTRACT The pGinger suite of expression plasmids comprises 43 plasmids that will enable precise constitutive and inducible gene expression in a wide range of Gram-negative bacterial species. Constitutive vectors are composed of 16 synthetic constitutive promoters upstream of red fluorescent protein (RFP), with a broad-host-range BBR1 origin and a kanamycin resistance marker. The family also has seven inducible systems (Jungle Express, PsaI/NahR, Pm/XylS, Prha/RhaS, LacO1/LacI, LacUV5/LacI, and Ptet/TetR) controlling RFP expression on BBR1/kanamycin plasmid backbones. For four of these inducible systems (Jungle Express, PsaI/NahR, LacO1/LacI, and Ptet/TetR), we created variants that utilize the RK2 origin and spectinomycin or gentamicin selection. Relevant RFP expression and growth data have been collected in the model bacterium *Escherichia coli* as well as *Pseudomonas putida*. All pGinger vectors are available via the Joint BioEnergy Institute (JBEI) Public Registry.

IMPORTANCE Metabolic engineering and synthetic biology are predicated on the precise control of gene expression. As synthetic biology expands beyond model organisms, more tools will be required that function robustly in a wide range of bacterial hosts. The pGinger family of plasmids constitutes 43 plasmids that will enable both constitutive and inducible gene expression in a wide range of nonmodel *Proteobacteria*.

KEYWORDS molecular genetics, plasmid, synthetic biology

Precise and reliable control over gene expression is one of the most fundamental requirements of synthetic and molecular biology (1). Consequently, there has been considerable effort toward identifying myriad genetic elements that enable researchers to regulate the strength and timing of transcription across all domains of life (2–4). The results of these efforts are often consolidated families of plasmid vectors that facilitate advanced genetic engineering, such as the BglBrick family of plasmids for *Escherichia coli* (5, 6) and the jStack vectors used in multiple plant species (7). However, as the field of synthetic biology moves beyond traditional model organisms, families of expression vectors must be tailored to meet the specific requirements of particular hosts. Advances in nonmodel organisms often come in the form of species- or genus-specific toolkits (8–10), though more recently, comprehensive plasmid toolkits have been developed and validated for a wide range of Gram-negative organisms (11). Resources such as the Standard European Vector Architecture (SEVA) platform provide repositories of standardized sequences and constructs (12, 13).

Editor Daniel R. Bond, University of Minnesota

Address correspondence to Jay D. Keasling, jdkeasling@lbl.gov, or Patrick M. Shih, pmshih@lbl.gov.

The authors declare a conflict of interest. J.D.K. has financial interests in Amyris, Ansa Biotechnologies, Apertor Pharma, Berkeley Yeast, Demetrix, Lygos, Napigen, ResVita Bio, and Zero Acre Farms.

Received 24 January 2023
Accepted 9 May 2023
Published 22 May 2023

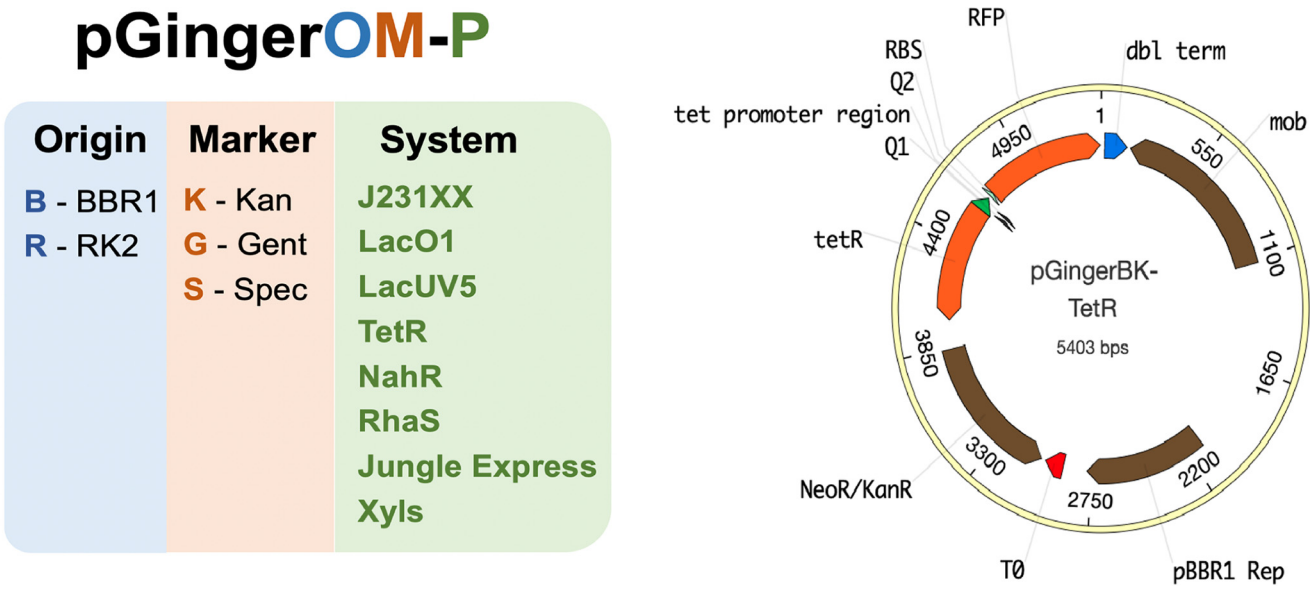

FIG 1 Plasmid architecture of the pGinger suite. The pGinger plasmids share a naming convention in which the first two letters after "pGinger" correspond to the origin and resistance marker, respectively, followed by the expression system. All plasmids share the same architecture as in the map of pGingerBK-TetR, whereby a conserved RBS-RFP is downstream of the promoter, followed by a strong terminator. All selectable markers are upstream of the promoter, with the origin between the marker and the RFP cassette.

Still, given that many bacteria require very particular combinations of promoters, origins, and selectable markers to enable controlled gene expression, there remains a need for vectors that will allow rapid prototyping of genetic circuits in understudied bacteria.

To facilitate the exploration of nonmodel hosts, we have developed a small suite of plasmids that permit both constitutive and inducible expression from the broad-host-range origin of replication BBR1 using a kanamycin selection marker. For a subset of the inducible systems that are known to work across multiple hosts, we have assembled combinatorial variants that utilize the compatible broad-host-range origin RK2 (14) as well as both spectinomycin and gentamicin selection markers. This family of plasmids, which we have named the pGinger suite, requires no assembly of these parts, can be easily cloned into via standard Gibson assembly techniques, and has both digital sequences and physical samples that can be publicly accessed through the Joint BioEnergy Institute (JBEI) registry (15).

RESULTS

Design and architecture of pGinger plasmids. All pGinger vectors express red fluorescent protein (RFP) with a consensus ribosomal binding site (RBS; TTTAAGAAGGAGATATACAT) derived from the BglBrick plasmid library. The overall conserved plasmid architecture and naming convention of the pGinger suite are shown in Fig. 1.

The BBR1 origin and kanamycin resistance cassette of relevant pGinger vectors were both derived from plasmid pBADTrfp (16). To develop a family of constitutive expression plasmids, the AraC coding sequence and promoter of pBADTrfp were replaced with 16 different synthetic promoters from the Anderson Promoter Library (http://parts.igem.org/Promoters/Catalog/Anderson). For the inducible vectors, the AraC coding sequence and promoter of pBADTrfp were replaced with the following seven inducible systems: Jungle Express, derived from pTR_sJExD-rfp (17); PsaI/NahR, derived from pPS43 (18); Prha/RhaS, derived from pCV203 (18); Ptet/TetR, derived from pBbE2a-RFP (6); Pm/XylS, derived from pPS66 (18); LacO1/LacI, derived from pBbE6a-RFP (6); and LacUV5/LacI, derived from pBbE5a-RFP (6). Three of these inducible systems, Pm/XylS, PsaI/NahR, and Prha/RhaS, utilize an activator or bifunctional transcription factor; the other systems feature transcriptional repressors. These BBR1 vectors contain the *mob* element that facilitates conjugal transfer. For four of the inducible systems (Jungle Express, PsaI/NahR, LacO1/LacI, and Ptet/TetR), additional vectors were constructed that varied both the origin and antibiotic marker. All RK2 origins were derived from pBb(RK2)1k-GFPuv (8), while the gentamicin resistance cassette was derived

TABLE 1 Plasmids in the pGinger suite[a]

Name	Origin	Marker	Promoter class	System	Inducer	JBEI ICE no.
pGingerBK-J23100	BBR1	Kanamycin	Constitutive	J23100	NA	JPUB_020797
pGingerBK-J23101	BBR1	Kanamycin	Constitutive	J23101	NA	JPUB_020799
pGingerBK-J23102	BBR1	Kanamycin	Constitutive	J23102	NA	JPUB_020815
pGingerBK-J23103	BBR1	Kanamycin	Constitutive	J23103	NA	JPUB_020801
pGingerBK-J23104	BBR1	Kanamycin	Constitutive	J23104	NA	JPUB_020803
pGingerBK-J23105	BBR1	Kanamycin	Constitutive	J23105	NA	JPUB_020817
pGingerBK-J23106	BBR1	Kanamycin	Constitutive	J23106	NA	JPUB_020793
pGingerBK-J23107	BBR1	Kanamycin	Constitutive	J23107	NA	JPUB_020819
pGingerBK-J23108	BBR1	Kanamycin	Constitutive	J23108	NA	JPUB_020821
pGingerBK-J23110	BBR1	Kanamycin	Constitutive	J23110	NA	JPUB_020805
pGingerBK-J23111	BBR1	Kanamycin	Constitutive	J23111	NA	JPUB_020807
pGingerBK-J23113	BBR1	Kanamycin	Constitutive	J23113	NA	JPUB_020809
pGingerBK-J23114	BBR1	Kanamycin	Constitutive	J13114	NA	JPUB_020811
pGingerBK-J23117	BBR1	Kanamycin	Constitutive	J13117	NA	JPUB_020795
pGingerBK-J23118	BBR1	Kanamycin	Constitutive	J23118	NA	JPUB_020823
pGingerBK-J23119	BBR1	Kanamycin	Constitutive	J23119	NA	JPUB_020813
pGingerBK-JE	BBR1	Kanamycin	Inducible	Jungle Express	Crystal violet	JPUB_020825
pGingerBK-NahR	BBR1	Kanamycin	Inducible	Psal/NahR	Salicylic acid	JPUB_020831
pGingerBK-RhaS	BBR1	Kanamycin	Inducible	Prha/RhaS	Rhamnose	JPUB_020829
pGingerBK-TetR	BBR1	Kanamycin	Inducible	Ptet/TetR	Oxytetracycline	JPUB_020835
pGingerBK-XylS	BBR1	Kanamycin	Inducible	Pm/XylS	Benzoate	JPUB_020827
pGingerBK-Lac	BBR1	Kanamycin	Inducible	LacO1/LacI	IPTG	JPUB_020833
pGingerBK-LacUV5	BBR1	Kanamycin	Inducible	LacUV5/LacI	IPTG	JPUB_020837
pGingerBG-JE	BBR1	Gentamicin	Inducible	Jungle Express	Crystal violet	JPUB_020847
pGingerBS-JE	BBR1	Spectinomycin	Inducible	Jungle Express	Crystal violet	JPUB_020855
pGingerRK-JE	RK2	Kanamycin	Inducible	Jungle Express	Crystal violet	JPUB_020871
pGingerRG-JE	RK2	Gentamicin	Inducible	Jungle Express	Crystal violet	JPUB_020881
pGingerRS-JE	RK2	Spectinomycin	Inducible	Jungle Express	Crystal violet	JPUB_020863
pGingerBG-NahR	BBR1	Gentamicin	Inducible	Psal/NahR	Salicylic acid	JPUB_020845
pGingerBS-NahR	BBR1	Spectinomycin	Inducible	Psal/NahR	Salicylic acid	JPUB_020853
pGingerRK-NahR	RK2	Kanamycin	Inducible	Psal/NahR	Salicylic acid	JPUB_020869
pGingerRG-NahR	RK2	Gentamicin	Inducible	Psal/NahR	Salicylic acid	JPUB_020879
pGingerRS-NahR	RK2	Spectinomycin	Inducible	Psal/NahR	Salicylic acid	JPUB_020859
pGingerBG-TetR	BBR1	Gentamicin	Inducible	Ptet/TetR	Oxytetracycline	JPUB_020843
pGingerBS-TetR	BBR1	Spectinomycin	Inducible	Ptet/TetR	Oxytetracycline	JPUB_020851
pGingerRK-TetR	RK2	Kanamycin	Inducible	Ptet/TetR	Oxytetracycline	JPUB_020865
pGingerRG-TetR	RK2	Gentamicin	Inducible	Ptet/TetR	Oxytetracycline	JPUB_020877
pGingerRS-TetR	RK2	Spectinomycin	Inducible	Ptet/TetR	Oxytetracycline	JPUB_020861
pGingerBG-LacO1	BBR1	Gentamicin	Inducible	LacO1/LacI	IPTG	JPUB_020841
pGingerBS-Lac	BBR1	Spectinomycin	Inducible	LacO1/LacI	IPTG	JPUB_020849
pGingerRK-LacO1	RK2	Kanamycin	Inducible	LacO1/LacI	IPTG	JPUB_020867
pGingerRG-LacO1	RK2	Gentamicin	Inducible	LacO1/LacI	IPTG	JPUB_020875
pGingerRS-LacO1	RK2	Spectinomycin	Inducible	LacO1/LacI	IPTG	JPUB_020857

[a]Relevant characteristics of pGinger plasmids, including origin of replication, antibiotic selection, promoter characteristics, and (if applicable) inducing molecule. JBEI public registry numbers are also included for digital accessibility. ICE, inventory of composable elements; NA, not applicable; IPTG, isopropyl-β-D-thiogalactopyranoside.

from pMQ30 (19) and the spectinomycin resistance cassette was derived from pSR43.6 (20). The RK2 vectors do not contain the *mob* element. A full description of each pGinger vector can be found in Table 1.

Evaluation of constitutive expression pGinger plasmids. To evaluate the relative strength of constitutive Anderson promoters in the context of the pGinger vectors, plasmids were introduced into both *Pseudomonas putida* and *E. coli*. Fluorescence was measured after growth in lysogeny broth (LB) medium for 24 h. When fluorescence was normalized to cell density, expression from Anderson promoters showed significant correlation (Spearman's $\rho = 0.49$; $P = 0.045$) between *P. putida* and *E. coli* (Fig. 2). Promoters J23103 and J23113 were significantly stronger in *E. coli* than in *P. putida*, while promoter J23111 was significantly stronger in *P. putida*. Promoter sequences and mean expression values in both *E. coli* and *P. putida* are listed in Table 2.

Evaluation of inducible pGinger plasmids. The expression of the seven inducible systems within the pGinger suite was evaluated using the BBR1 origin and kanamycin marker (pGingerBK) against a titration of the inducer in both *E. coli* and *P. putida* (Fig. 3). All systems

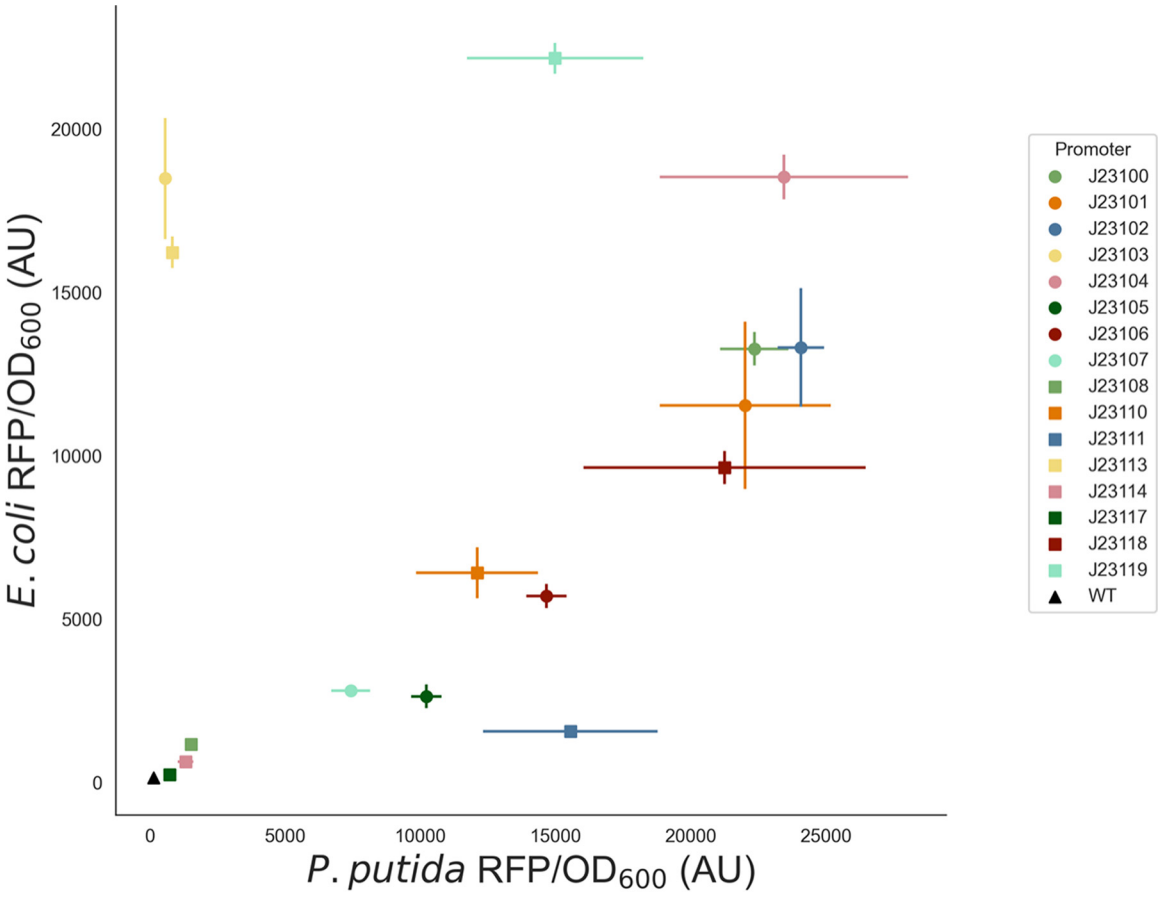

FIG 2 Activity of constitutive promoters in *E. coli* and *P. putida*. RFP expression normalized to cell density from Anderson promoters within either *E. coli* (*y* axis) or *P. putida* (*x* axis) is shown with standard deviations (n = 3). The background fluorescence of the two bacteria is indicated by "WT" (wild type). Optical density measurements are shown in Fig. S1 in the supplemental material. AU, arbitrary units.

showed inducibility in *E. coli*, and all but the rhamnose-inducible system Prha/RhaS showed inducibility in *P. putida*. Relevant expression characteristics of the inducible pGingerBK vectors in both tested bacteria are listed in Table 3. The strongest normalized expression from an inducible system in *E. coli* was the Ptet/TetR system, while both the strongest in *P. putida* were found to be Psal/NahR and Jungle Express inducible systems, which showed nearly identical

TABLE 2 Expression of pGinger Anderson promoters[a]

Promoter	Promoter sequence	*E. coli* expression	*P. putida* expression
J23100	TTGACGGCTAGCTCAGTCCTAGGTACAGTGCTAGC	13,267 (±517)	22,343 (±1,262)
J23101	TTTACAGCTAGCTCAGTCCTAGGTATTATGCTAGC	11,530 (±2,565)	22,010 (±3,162)
J23102	TTGACAGCTAGCTCAGTCCTAGGTACTGTGCTAGC	13,300 (±1,815)	24,067 (±858)
J23103	CTGATAGCTAGCTCAGTCCTAGGGATTATGCTAGC	18,476 (±1,857)	565 (±135)
J23104	TTGACAGCTAGCTCAGTCCTAGGTATTGTGCTAGC	18,522 (±682)	23,440 (±4,588)
J23105	TTTACGGCTAGCTCAGTCCTAGGTACTATGCTAGC	2,622 (±363)	10,220 (±558)
J23106	TTTACGGCTAGCTCAGTCCTAGGTATAGTGCTAGC	5,697 (±369)	14,659 (±748)
J23107	TTTACGGCTAGCTCAGCCCTAGGTATTATGCTAGC	2,798 (±44)	7,429 (±716)
J23108	CTGACAGCTAGCTCAGTCCTAGGTATAATGCTAGC	1,149 (±84)	1,523 (±84)
J23110	TTTACGGCTAGCTCAGTCCTAGGTACAATGCTAGC	6,402 (±782)	12,098 (±2,251)
J23111	TTGACGGCTAGCTCAGTCCTAGGTATAGTGCTAGC	1,547 (±106)	15,548 (±3,229)
J23113	CTGATGGCTAGCTCAGTCCTAGGGATTATGCTAGC	16,220 (±480)	826 (±92)
J23114	TTTATGGCTAGCTCAGTCCTAGGTACAATGCTAGC	625 (±48)	1,325 (±289)
J23117	TTGACAGCTAGCTCAGTCCTAGGGATTGTGCTAGC	229 (±25)	730 (±28)
J23118	TTGACGGCTAGCTCAGTCCTAGGTATTGTGCTAGC	9,628 (±507)	21,237 (±5,215)
J23119	TTGACAGCTAGCTCAGTCCTAGGTATAATGCTAGC	22,157 (±473)	14,979 (±3,262)
WT	NA	124 (±6)	141 (±17)

[a]For each Anderson promoter, the sequence is provided as well as the mean cell density-normalized RFP fluorescence in both *E. coli* and *P. putida*. Standard deviations are provided in parentheses (n = 3). The background fluorescence of *E. coli* is indicated by "WT" (wild type).

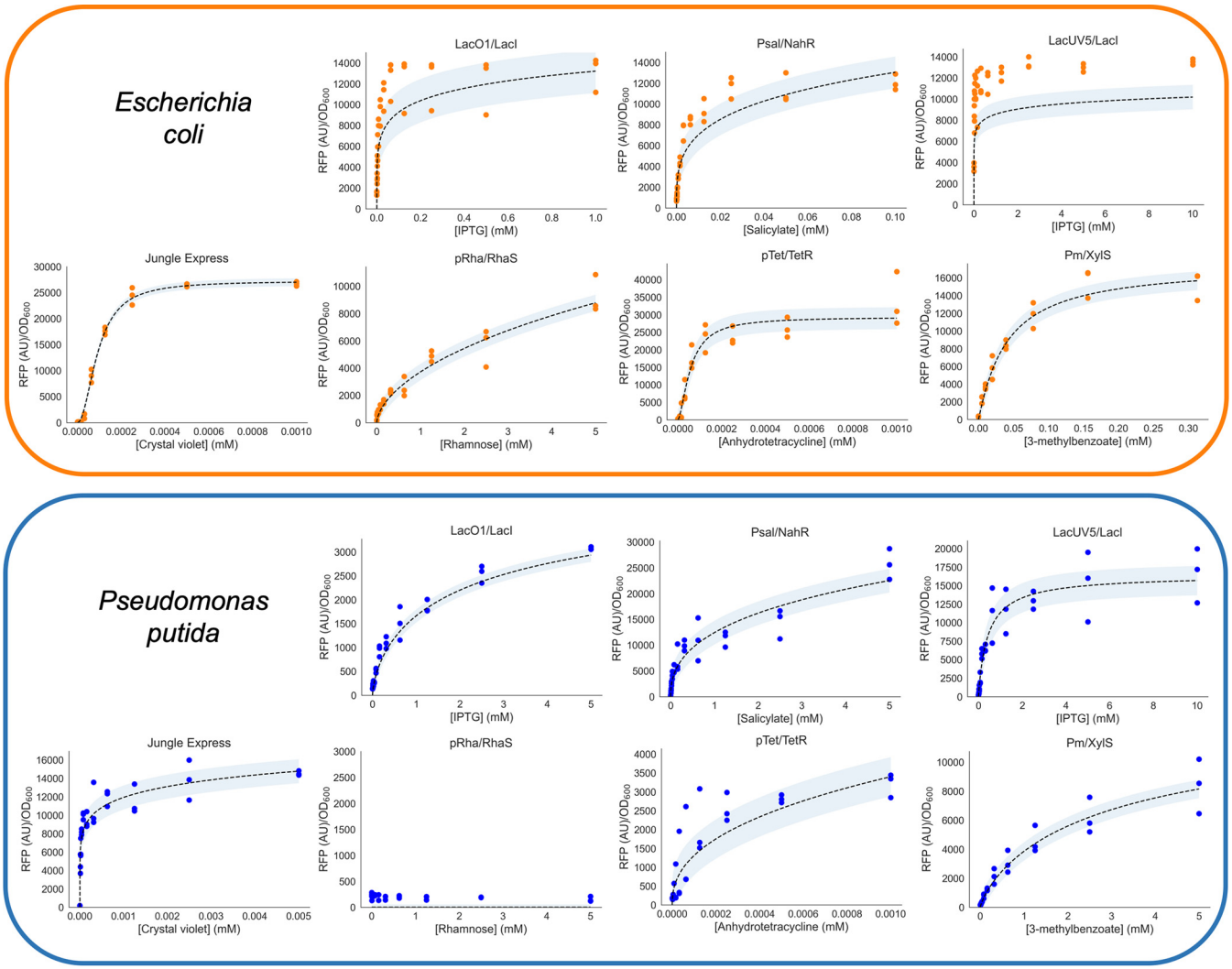

FIG 3 Activity of inducible systems in *E. coli* and *P. putida*. RFP expression normalized to cell density (*y* axis) from inducible systems within either *E. coli* (top panel in orange) or *P. putida* (bottom panel in blue) is shown as a function of millimolar concentration of inducer (*x* axis). Fits to the Hill equation are shown as dashed lines and shaded to show confidence intervals. Raw data points are overlaid ($n = 3$). Corresponding optical density measurements are shown in Fig. S2.

maximal expression. In both bacteria, the Jungle Express system demonstrated the greatest level of induction relative to background expression.

To evaluate the effects of various origin and selectable markers on expression from inducible systems, all six variants of Jungle Express, LacO1/LacI, Psal/NahR, and Ptet/TetR were investigated for their dose responses to their inducer molecules in *E. coli* (Fig. 4). Relevant expression parameters are listed in Table 4. In general, BBR1 variants showed greater expression than RK2 origin plasmids, which was expected given the higher copy number of BBR1 plasmids in *E. coli* (11). Among the pGinger Jungle Express vectors, both pGingerRS-JE and pGingerRK-JE showed dose responses distinct from those of the other vectors (Fig. 4, top left). Notably, all pGingerRS (RK2-spectinomycin) plasmids showed the lowest expression across each system tested (Table 4).

DISCUSSION

The pGinger suite of plasmids offers researchers an array of small, preassembled vectors that will permit rapid identification of useful genetic elements in diverse Gram-negative bacteria due to the use of broad-host-range origins (RK2) and selectable markers known to work across many species (kanamycin, spectinomycin, and gentamicin). The compatibility of RK2 and BBR1 origins may also permit researchers to introduce multiple pGinger vectors into a single

TABLE 3 Inducible systems in *E. coli* and *P. putida*[a]

System	Organism	Background	Max expression	Max concn	Induction
LacO1/LacI	*E. coli*	1,510 (±186)	13,127 (±1,693)	1 mM	9×
	P. putida	137 (±5)	3,074 (±30)	5 mM	22×
PsaI/NahR	*E. coli*	762 (±130)	12,051 (±759)	100 μM	16×
	P. putida	237 (±5)	25,697 (±2,976)	5 mM	108×
LacUV5/LacI	*E. coli*	3,577 (±36)	10,137 (±855)	10 mM	4×
	P. putida	203 (±53)	16,622 (±3,671)	10 mM	82×
Jungle Express	*E. coli*	104 (±7)	26,717 (±418)	1 μM	257×
	P. putida	176 (±5)	14,552 (±145)	2.5 μM	83×
Prha/RhaS	*E. coli*	172 (±42)	9,251 (±1,389)	5 mM	54×
	P. putida	NA	NA	NA	NA
Ptet/TetR	*E. coli*	341 (±10)	33,631 (±7,692)	1 μM	98×
	P. putida	176 (±9)	3,214 (±319)	1 μM	18×
Pm/XylS	*E. coli*	329 (±57)	15,280 (±1,590)	313 μM	46×
	P. putida	161 (±7)	8,401 (±1,877)	5 mM	52×

[a]For each inducible system on a BBR1 origin with a kanamycin marker, the experimentally observed background (uninduced) fluorescence and maximal fluorescence are given for both *E. coli* and *P. putida*. Standard deviations are provided in parentheses (n = 3). Additionally, the inducer concentration used to achieve maximal expression and the relative induction levels are listed. Max, maximum.

strain simultaneously (14). In combination with other recent plasmid suites that have been publicly released, the pGinger plasmids have the potential to facilitate more advanced synthetic biology and metabolic engineering efforts in bacterial species that have been traditionally understudied.

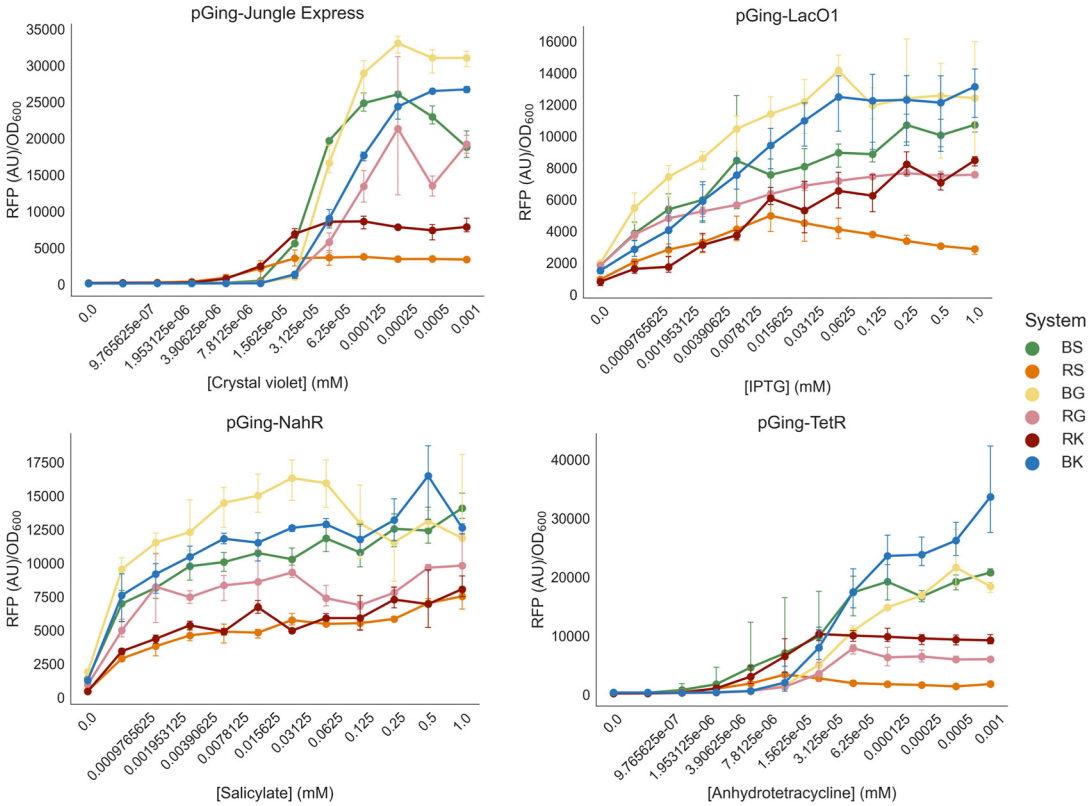

FIG 4 Activity of inducible pGinger variants in *E. coli*. For origin and selection marker pGinger variants of Jungle Express (top left), LacO1/LacI (top right), PsaI/NahR (bottom left), and pTet/TetR (bottom right), dose-response curves of normalized RFP expression are shown as a function of millimolar concentration of inducer. Error bars represent standard deviations (n = 3). Note that the x axis is nonlinear. Corresponding optical density measurements are shown in Fig. S3. Results of kinetic experiments for these systems are shown in Fig. S4 to S7.

TABLE 4 Inducible pGinger variants in *E. coli*[a]

System	Origin	Marker	Background	Max expression	Max concn	Induction
LacO1/LacI	BBR1	Kan	1,510 (±186)	13,127 (±1,693)	1 mM	9×
LacO1/LacI	BBR1	Gent	1,976 (±70)	14,143 (±1,608)	63 μM	7×
LacO1/LacI	BBR1	Spec	1,830 (±320)	10,694 (±943)	250 μM	6×
LacO1/LacI	RK2	Kan	803 (±216)	8,213 (±721)	250 μM	10×
LacO1/LacI	RK2	Gent	1,823 (±78)	7,654 (±230)	250 μM	4×
LacO1/LacI	RK2	Spec	950 (±46)	4,967 (±895)	16 μM	5×
Psal/NahR	BBR1	Kan	1,260 (±57)	16,484 (±1,693)	500 μM	9×
Psal/NahR	BBR1	Gent	1,877 (±334)	16,317 (±1,534)	31 μM	9×
Psal/NahR	BBR1	Spec	1,372 (±84)	14,083 (±984)	1 mM	10×
Psal/NahR	RK2	Kan	445 (±39)	8,048 (±859)	1 mM	18×
Psal/NahR	RK2	Gent	934 (±56)	9,299 (±460)	1 mM	10×
Psal/NahR	RK2	Spec	482 (±69)	7,510 (±817)	1 mM	16×
Jungle Express	BBR1	Kan	104 (±6)	267,175 (±418)	1 μM	257×
Jungle Express	BBR1	Gent	136 (±19)	33,060 (±1,185)	250 nM	243×
Jungle Express	BBR1	Spec	152 (±5)	26,039 (±355)	250 nM	171×
Jungle Express	RK2	Kan	163 (±27)	8,616 (±902)	125 nM	52×
Jungle Express	RK2	Gent	138 (±51)	21,314 (±9,517)	250 nM	155×
Jungle Express	RK2	Spec	168 (±5)	3,763 (±204)	125 nM	22×
Ptet/TetR	BBR1	Kan	341 (±10)	33,631 (±7,692)	1 μM	98×
Ptet/TetR	BBR1	Gent	351 (±32)	21,646 (±5,579)	500 nM	62×
Ptet/TetR	BBR1	Spec	232 (±43)	19,224 (±3,027)	125 nM	83×
Ptet/TetR	RK2	Kan	184 (±5)	10,281 (±967)	31 nM	56×
Ptet/TetR	RK2	Gent	232 (±39)	7,883 (±865)	63 nM	34×
Ptet/TetR	RK2	Spec	197 (±5)	3,399 (±143)	16 nM	17×

[a]For pGinger variants of LacO1/LacI, Psal/NahR, Jungle Express, and Ptet/TetR inducible systems, the experimentally observed background (uninduced) fluorescence and maximal fluorescence in *E. coli* are provided. Standard deviations are provided in parentheses (n = 3). Additionally, the inducer concentration used to achieve maximal expression and the relative induction levels are listed. Kan, kanamycin; Gent, gentamicin; Spec, spectinomycin.

MATERIALS AND METHODS

Strains and media. Cultures were grown in lysogeny broth (LB) Miller medium (BD Biosciences, USA) at 37°C for *E. coli* XL1-Blue (QB3 MacroLab, USA) and 30°C for *P. putida* KT2440 (ATCC 47054). The medium was supplemented with kanamycin (50 mg/L; Sigma-Aldrich, USA), gentamicin (30 mg/L; Fisher Scientific, USA), or spectinomycin (100 mg/L; Sigma-Aldrich), when indicated. All other compounds were purchased through Sigma-Aldrich.

Plasmid design and construction. All plasmids were designed using Device Editor and Vector Editor software, while all primers used for the construction of plasmids were designed using j5 software (15, 21, 22). Plasmids were assembled via Gibson assembly using standard protocols (23). Plasmids were routinely isolated using the Qiaprep Spin miniprep kit (Qiagen, USA), and all primers were purchased from Integrated DNA Technologies (IDT; Coralville, IA). The fluorescent protein used in all plasmids was mRFP1 (24).

Characterization assays. To characterize RFP expression from the vectors, we measured optical density and fluorescence after growth in 96-well plates for 24 h. First, overnight cultures were inoculated into 5 mL of LB medium from single colonies and grown at 30°C or 37°C. These cultures were then diluted 1:100 into 500 μL of LB medium with the appropriate antibiotic in 96 square v-bottom deep-well plates (Biotix DP22009CVS). For characterization of the inducible systems, inducer was added to wells in the first column of the plate at the maximum concentration tested and diluted 2-fold across the plate until the last column, which was left as the zero-inducer control. Plates were sealed with a gas-permeable microplate adhesive film (Axygen BF400S) and cultures were grown for 24 h at either 30°C or 37°C with shaking at 200 rpm. Optical density was measured at 600 nm, and fluorescence was measured at an excitation wavelength of 535 nm and an emission wavelength of 620 nm. All data were analyzed and visualized using custom Python scripts using the SciPy (25), NumPy (26), Pandas, Matplotlib, and Seaborn libraries. Fits to the Hill equation were done as previously described (27).

Plasmid and sequence availability. All strains and plasmid sequences from Table 1 can be found via the following link to the JBEI Public Registry: https://public-registry.jbei.org/folders/771. Users can request strains via an material transfer agreement (MTA).

SUPPLEMENTAL MATERIAL

Supplemental material is available online only.

SUPPLEMENTAL FILE 1, DOCX file, 3.2 MB.

ACKNOWLEDGMENTS

Mitchell G. Thompson is a Simons Foundation Awardee of the Life Sciences Research Foundation. Lucas M. Waldburger is funded by the National Science Foundation Graduate

Research Fellowship. This work was part of the DOE Joint BioEnergy Institute (https://www.jbei.org), supported by the U.S. Department of Energy, Office of Science, Office of Biological and Environmental Research, supported by the U.S. Department of Energy, Energy Efficiency and Renewable Energy, Bioenergy Technologies Office, through contract DE-AC02-05CH11231 between Lawrence Berkeley National Laboratory and the U.S. Department of Energy. The views and opinions of the authors expressed herein do not necessarily state or reflect those of the U.S. Government or any agency thereof. Neither the U.S. Government nor any agency thereof, nor any of their employees, makes any warranty, expressed or implied, or assumes any legal liability or responsibility for the accuracy, completeness, or usefulness of any information, apparatus, product, or process disclosed, or represents that its use would not infringe privately owned rights. The Department of Energy will provide public access to these results of federally sponsored research in accordance with the DOE Public Access Plan (http://energy.gov/downloads/doe-public-access-plan).

Conceptualization, A.N.P. and M.G.T.; Methodology, A.N.P. and M.G.T.; Investigation, A.N.P., M.G.T., L.D.K., C.H., K.M.V., and L.M.W.; Writing – Original Draft, A.N.P. and M.G.T.; Writing – Review and Editing, all authors; Resources and Supervision, P.M.S. and J.D.K.

J.D.K. has financial interests in Amyris, Ansa Biotechnologies, Apertor Pharma, Berkeley Yeast, Demetrix, Lygos, Napigen, ResVita Bio, and Zero Acre Farms.

REFERENCES

1. Khalil AS, Collins JJ. 2010. Synthetic biology: applications come of age. Nat Rev Genet 11:367–379. https://doi.org/10.1038/nrg2775.
2. Nielsen AAK, Segall-Shapiro TH, Voigt CA. 2013. Advances in genetic circuit design: novel biochemistries, deep part mining, and precision gene expression. Curr Opin Chem Biol 17:878–892. https://doi.org/10.1016/j.cbpa.2013.10.003.
3. Zhang Y, Ding W, Wang Z, Zhao H, Shi S. 2021. Development of host-orthogonal genetic systems for synthetic biology. Adv Biol (Weinh) 5:e2000252. https://doi.org/10.1002/adbi.202000252.
4. Johns NI, Gomes ALC, Yim SS, Yang A, Blazejewski T, Smillie CS, Smith MB, Alm EJ, Kosuri S, Wang HH. 2018. Metagenomic mining of regulatory elements enables programmable species-selective gene expression. Nat Methods 15:323–329. https://doi.org/10.1038/nmeth.4633.
5. Anderson JC, Dueber JE, Leguia M, Wu GC, Goler JA, Arkin AP, Keasling JD. 2010. BglBricks: a flexible standard for biological part assembly. J Biol Eng 4:1. https://doi.org/10.1186/1754-1611-4-1.
6. Lee TS, Krupa RA, Zhang F, Hajimorad M, Holtz WJ, Prasad N, Lee SK, Keasling JD. 2011. BglBrick vectors and datasheets: a synthetic biology platform for gene expression. J Biol Eng 5:12. https://doi.org/10.1186/1754-1611-5-12.
7. Shih PM, Vuu K, Mansoori N, Ayad L, Louie KB, Bowen BP, Northen TR, Loqué D. 2016. A robust gene-stacking method utilizing yeast assembly for plant synthetic biology. Nat Commun 7:13215. https://doi.org/10.1038/ncomms13215.
8. Cook TB, Rand JM, Nurani W, Courtney DK, Liu SA, Pfleger BF. 2018. Genetic tools for reliable gene expression and recombineering in Pseudomonas putida. J Ind Microbiol Biotechnol 45:517–527. https://doi.org/10.1007/s10295-017-2001-5.
9. Phelan RM, Sachs D, Petkiewicz SJ, Barajas JF, Blake-Hedges JM, Thompson MG, Reider Apel A, Rasor BJ, Katz L, Keasling JD. 2017. Development of next generation synthetic biology tools for use in Streptomyces venezuelae. ACS Synth Biol 6:159–166. https://doi.org/10.1021/acssynbio.6b00202.
10. Calero P, Nikel PI. 2019. Chasing bacterial chassis for metabolic engineering: a perspective review from classical to non-traditional microorganisms. Microb Biotechnol 12:98–124. https://doi.org/10.1111/1751-7915.13292.
11. Schuster LA, Reisch CR. 2021. A plasmid toolbox for controlled gene expression across the Proteobacteria. Nucleic Acids Res 49:7189–7202. https://doi.org/10.1093/nar/gkab496.
12. Martínez-García E, Fraile S, Algar E, Aparicio T, Velázquez E, Calles B, Tas H, Blázquez B, Martín B, Prieto C, Sánchez-Sampedro L, Nørholm MHH, Volke DC, Wirth NT, Dvořák P, Alejaldre L, Grozinger L, Crowther M, Goñi-Moreno A, Nikel PI, Nogales J, de Lorenzo V. 2023. SEVA 4.0: an update of the Standard European Vector Architecture database for advanced analysis and programming of bacterial phenotypes. Nucleic Acids Res 51:D1558–D1567. https://doi.org/10.1093/nar/gkac1059.
13. Martínez-García E, de Lorenzo V. 2017. Molecular tools and emerging strategies for deep genetic/genomic refactoring of Pseudomonas. Curr Opin Biotechnol 47:120–132. https://doi.org/10.1016/j.copbio.2017.06.013.
14. Pasin F, Bedoya LC, Bernabé-Orts JM, Gallo A, Simón-Mateo C, Orzaez D, García JA. 2017. Multiple T-DNA delivery to plants using novel mini binary vectors with compatible replication origins. ACS Synth Biol 6:1962–1968. https://doi.org/10.1021/acssynbio.6b00354.
15. Ham TS, Dmytriv Z, Plahar H, Chen J, Hillson NJ, Keasling JD. 2012. Design, implementation and practice of JBEI-ICE: an open source biological part registry platform and tools. Nucleic Acids Res 40:e141. https://doi.org/10.1093/nar/gks531.
16. Bi C, Su P, Müller J, Yeh Y-C, Chhabra SR, Beller HR, Singer SW, Hillson NJ. 2013. Development of a broad-host synthetic biology toolbox for Ralstonia eutropha and its application to engineering hydrocarbon biofuel production. Microb Cell Fact 12:107. https://doi.org/10.1186/1475-2859-12-107.
17. Ruegg TL, Pereira JH, Chen JC, DeGiovanni A, Novichkov P, Mutalik VK, Tomaleri GP, Singer SW, Hillson NJ, Simmons BA, Adams PD, Thelen MP. 2018. Jungle Express is a versatile repressor system for tight transcriptional control. Nat Commun 9:3617. https://doi.org/10.1038/s41467-018-05857-3.
18. Calero P, Jensen SI, Nielsen AT. 2016. Broad-host-range ProUSER vectors enable fast characterization of inducible promoters and optimization of *p*-coumaric acid production in *Pseudomonas putida* KT2440. ACS Synth Biol 5:741–753. https://doi.org/10.1021/acssynbio.6b00081.
19. Shanks RMQ, Kadouri DE, MacEachran DP, O'Toole GA. 2009. New yeast recombineering tools for bacteria. Plasmid 62:88–97. https://doi.org/10.1016/j.plasmid.2009.05.002.
20. Schmidl SR, Sheth RU, Wu A, Tabor JJ. 2014. Refactoring and optimization of light-switchable Escherichia coli two-component systems. ACS Synth Biol 3:820–831. https://doi.org/10.1021/sb500273n.
21. Chen J, Densmore D, Ham TS, Keasling JD, Hillson NJ. 2012. DeviceEditor visual biological CAD canvas. J Biol Eng 6:1. https://doi.org/10.1186/1754-1611-6-1.
22. Hillson NJ, Rosengarten RD, Keasling JD. 2012. j5 DNA assembly design automation software. ACS Synth Biol 1:14–21. https://doi.org/10.1021/sb2000116.
23. Gibson DG, Young L, Chuang R-Y, Venter JC, Hutchison CA, Smith HO. 2009. Enzymatic assembly of DNA molecules up to several hundred kilobases. Nat Methods 6:343–345. https://doi.org/10.1038/nmeth.1318.
24. Campbell RE, Tour O, Palmer AE, Steinbach PA, Baird GS, Zacharias DA, Tsien RY. 2002. A monomeric red fluorescent protein. Proc Natl Acad Sci U S A 99:7877–7882. https://doi.org/10.1073/pnas.082243699.
25. Virtanen P, Gommers R, Oliphant TE, Haberland M, Reddy T, Cournapeau D, Burovski E, Peterson P, Weckesser W, Bright J, van der Walt SJ, Brett M, Wilson J, Millman KJ, Mayorov N, Nelson ARJ, Jones E, Kern R, Larson E, Carey CJ, Polat İ, Feng Y, Moore EW, VanderPlas J, Laxalde D, Perktold J, Cimrman R, Henriksen I, Quintero EA, Harris CR, Archibald AM, Ribeiro AH,

Pedregosa F, van Mulbregt P, SciPy 1.0 Contributors. 2020. SciPy 1.0: fundamental algorithms for scientific computing in Python. Nat Methods 17:261–272. https://doi.org/10.1038/s41592-019-0686-2.
26. van der Walt S, Colbert SC, Varoquaux G. 2011. The NumPy array: a structure for efficient numerical computation. Comput Sci Eng 13:22–30. https://doi.org/10.1109/MCSE.2011.37.
27. Thompson MG, Costello Z, Hummel NFC, Cruz-Morales P, Blake-Hedges JM, Krishna RN, Skyrud W, Pearson AN, Incha MR, Shih PM, Garcia-Martin H, Keasling JD. 2019. Robust characterization of two distinct glutarate sensing transcription factors of Pseudomonas putida L-lysine metabolism. ACS Synth Biol 8:2385–2396. https://doi.org/10.1021/acssynbio.9b00255.